Applied Physics Letters

Demonstration of mechanically exfoliated #-Ga_2O_3/GaN p-n heterojunction

Cite as: Appl. Phys. Lett. **114**, 162103 (2019); https://doi.org/10.1063/1.5088516
Submitted: 10 January 2019 . Accepted: 27 March 2019 . Published Online: 25 April 2019

Jossue Montes, Chen Yang, Houqiang Fu, Tsung-Han Yang, Kai Fu, Hong Chen, Jingan Zhou, Xuanqi Huang, and Yuji Zhao

AIP Publishing

Applied Physics Letters ARTICLE scitation.org/journal/apl

Demonstration of mechanically exfoliated β-Ga_2O_3/GaN p-n heterojunction

Cite as: Appl. Phys. Lett. **114**, 162103 (2019); doi: 10.1063/1.5088516
Submitted: 10 January 2019 · Accepted: 27 March 2019 ·
Published Online: 25 April 2019

Jossue Montes,[a),b)] Chen Yang,[a),b)] Houqiang Fu, Tsung-Han Yang, Kai Fu, Hong Chen, Jingan Zhou, Xuanqi Huang, and Yuji Zhao[b)]

AFFILIATIONS

School of Electrical, Computer, and Energy Engineering, Arizona State University, Tempe, Arizona 85281, USA

[a)]**Contributions:** J. Montes and C. Yang contributed equally to this work.
[b)]**Electronic addresses:** jossue.montes@asu.edu; cyang130@asu.edu; and yuji.zhao@asu.edu

ABSTRACT

This work demonstrates the construction of p-n heterojunctions between mechanically exfoliated beta-phase gallium oxide (β-Ga_2O_3) and p-GaN. The detailed mechanical exfoliation process was developed and can be used for further device applications. The atomic force microscopy study showed that the exfoliated β-Ga_2O_3 flakes had a very smooth surface with a roughness of 0.65 nm. Transmission electron microscopy revealed a clearly defined interface between the exfoliated β-Ga_2O_3 and p-GaN. The p-n heterojunction exhibited a turn-on voltage of 3.6 V and a rectification ratio of $\sim 10^5$. The heterojunction also showed good thermal performance up to 200 °C. Ideality factors and turn-on voltages decrease with temperature, tending toward the ideal threshold voltage of 3.2 V as determined by Silvaco simulations. This work provides valuable information on a mechanically exfoliated β-Ga_2O_3/GaN p-n heterojunction, which opens up the opportunities for a variety of photonic and electronic applications.

Beta-phase gallium oxide (β-Ga_2O_3) is an attractive ultrawide bandgap (UWBG) semiconductor with a bandgap of 4.6–4.9 eV, which enables deep ultraviolet (DUV)[1,2] and high-power[3] applications. With a high breakdown electric field of 8 MV/cm, a high saturation electron velocity of 2×10^7 cm/s, and a large Baliga's figure of merit (BFOM),[4–9] β-Ga_2O_3 shows tremendous potential to outperform current high-power semiconductors such as GaN and SiC. Like most other UWBG materials,[10] β-Ga_2O_3 also shows promise in harsh-environment applications, i.e., operating under radiation hazards and high temperatures.[11] Remarkably high interest in research on β-Ga_2O_3 has arisen not only from the ready availability of large, low-cost, high-quality wafers of bulk β-Ga_2O_3[10] but also from its unique material properties due to its monoclinic crystal structure. β-Ga_2O_3 is a 3D crystal that belongs to the C2/m space group with lattice constants $\boldsymbol{a} = 1.22$ nm, $\boldsymbol{b} = 0.303$ nm, and $\boldsymbol{c} = 0.580$ nm, and angle $\beta = 103.8°$.[12] The unit cell of β-Ga_2O_3 contains 3 crystallographically unique oxygen atoms and 2 gallium atoms. The result of this arrangement is a strong chemical, electrical, and thermal anisotropy.[6] The two gallium positions comprise tetrahedral and octahedral arrangements, where the latter arrangement is situated parallel to the (010) plane. This results in not only a significantly longer $\boldsymbol{a}$ lattice constant but also strong cleavage planes parallel to the (100) and (001) planes, which permit a cleaving or mechanical exfoliation of thin flakes. The exfoliated layers may then be transferred to any arbitrary substrates. This process is similar to that done on 2D materials like graphene, for which the 2010 Nobel prize was awarded,[13] and transition metal dichalcogenides (TMDs) such as MoS_2 and WSe_2.[14,15]

The mechanical exfoliation of β-Ga_2O_3 has opened up the prospect of a great number of devices.[16–18] Very recently, electronic and optoelectronic devices constructed from mechanically exfoliated β-Ga_2O_3 flakes have enjoyed considerable attention, including diodes,[19] transistors,[20–26] and photodetectors.[1,18,27,28] However, the full breadth of potential devices has yet to be demonstrated because effective p-doping in β-Ga_2O_3 is still not fully realized due to the absence of suitable shallow acceptors.[29,30] Another reason is the character of the valence band states in β-Ga_2O_3: they are characterized as having small dispersion, large effective masses, and high density of states, which lead to highly localized and low mobility holes.[31–34] On the other hand, after decades of development, p-type doping is now readily available in the wide bandgap (WBG) semiconductor GaN. It is also shown that GaN can be epitaxially grown on $(\bar{2}\ 01)$ β-Ga_2O_3 due to the symmetry match.[35] Therefore, bipolar devices between β-Ga_2O_3 and GaN are an appealing consideration. In this work, we report the construction of a p-n heterojunction between mechanically

exfoliated n-type β-Ga_2O_3 and p-type GaN. The heterojunction shows decent rectifying behaviors with a turn-on voltage of 3.6 V and an on/off ratio of 10^5. The turn-on voltage and ideality factor improved with increasing temperatures from 25 °C to 200 °C. By controlling the exfoliation process, we fabricated a p-n heterojunction with different β-Ga_2O_3 thicknesses, and the device characteristics with respect to the β-Ga_2O_3 thickness were also analyzed.

The p-type GaN layer was grown by metalorganic chemical deposition (MOCVD) on GaN substrates. p-GaN had a thickness of 500 nm and a doping concentration of 10^{19} cm^{-3}, on top of a GaN buffer layer. The precursors for Ga and N were trimethylgallium (TMGa) and ammonia (NH_3), respectively. The p-type dopants were Mg from bis(cyclopentadienyl)magnesium (Cp_2Mg). After the growth, p-GaN was cleaned in acetone and isopropyl alcohol (IPA) for 5 min each under ultrasonic agitation in order to remove any residual organic contamination on the surface. Metal stacks of Pd (30 nm)/Ni (20 nm)/Au (150 nm) were deposited using electron beam evaporation on p-GaN and annealed under N_2 at 450 °C for 30 s to form the p-contact. 2-in. ($\bar{2}$ 01) β-Ga_2O_3 bulk substrates were purchased from Tamura Corporation with a thickness of 650 μm and a Sn doping of 5×10^{18} cm^{-3}. They were grown by the edge-defined film-fed growth (EFG) method. More information about the growth can be found elsewhere.[6,8] Figure 1 shows the fabrication process flow of the β-Ga_2O_3/GaN p-n heterojunction. The bulk ($\bar{2}$ 01) β-Ga_2O_3 wafers were cleaved with a diamond tip parallel to the wafer flat. Doing so exposes the (100) plane. Flakes of varying thicknesses, which comprise the (100) plane, can be easily removed from the freshly cleaved bulk wafer using tweezers [Fig. 1(a)]. Using electron beam evaporation, metal stacks of Ti (20 nm)/Al (30 nm)/Ni (20 nm)/Au (100 nm) were deposited on the cleaved β-Ga_2O_3 fragment to form the n-contact [Fig. 1(b)]. The contact was subsequently annealed in N_2 at 470 °C for 1 min [Fig. 1(c)]. The metal-semiconductor stack was placed upside down on Revalpha Heat Release tape (#3193MS) with the β-Ga_2O_3 exposed [Fig. 1(d)]. Regular Scotch tape was used to peel off layers of β-Ga_2O_3 from the bulk, reducing the thickness over many exfoliations [Fig. 1(e)]. After the final exfoliation with Scotch tape, the β-Ga_2O_3, metal, and thermal tape stack was then immediately transferred to the p-GaN substrate [Fig. 1(f)]. The backside of the tape was pressed down firmly on the p-GaN substrate. At this step, β-Ga_2O_3 will adhere onto p-GaN by its own pseudo-van der Waals attractive forces. The entire structure was placed upside down on a hot plate set to 120 °C with vacuum seal beneath [Fig. 1(g)]. The upside down placement and vacuum seal are to ensure that heat is evenly distributed and that the adhesion strength of the tape evenly decreases across the area of the tape. After 2 min, the adhesive strength of the thermal tape vanishes completely, and the stack may be separated cleanly from the tape. Mechanical exfoliation by this method will result in β-Ga_2O_3 flakes ranging between tens of nanometers to over 100 μm thickness, depending on the number of times peeling off is performed.

Atomic force microscopy (AFM) was performed using a Bruker Multimode instrument to examine the surface roughness of the exfoliated flakes [Figs. 2(a) and 2(b)]. The root-mean-square roughness was 0.65 nm in a 5×5 μm scanning area, which is comparable to previous studies.[22] Figure 2(c) shows the height profile of an 80 nm-thick exfoliated flake. The inset shows an optical microscopy image of the as-transferred flake. High resolution x-ray diffraction (HR-XRD) was performed on the as-received β-Ga_2O_3 to examine the crystal quality

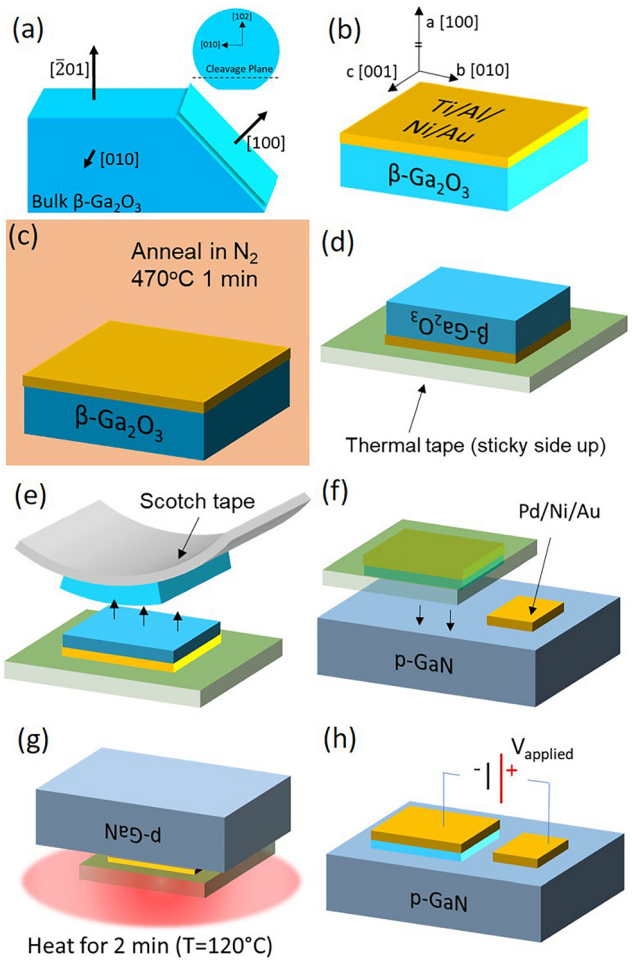

FIG. 1. Mechanical exfoliation of β-Ga_2O_3. (a) The bulk ($\bar{2}$ 01) wafers of β-Ga_2O_3 can be cleaved to expose the (100) plane. (b) Metal deposition via electron beam evaporation to deposit the n contact on β-Ga_2O_3. (c) Anneal the contact in high-purity N_2 at 470 °C for 1 min. (d) Thermal tape is placed over the β-Ga_2O_3, metal stack and turned upside down. (e) Ordinary scotch tape is placed sticky side-down over the exposed β-Ga_2O_3 and peeled off, removing layers of the β-Ga_2O_3. (f) The β-Ga_2O_3, metal, thermal tape is placed on p-type GaN, which had a p-contact deposited beforehand. (g) The entire stack is placed upside down on a vacuum-sealed hot plate at 120 °C for 2 min to evenly distribute the heat across the thermal tape. (h) The finished device.

[Fig. 2(d)]. The measurements were carried out with a PANalytical X'Pert Pro diffractometer using the Cu Kα1 radiation as the X-ray source, a hybrid monochromator for the incident beam optics, and a triple axis module for diffracted beam optics. The full-width at half-maximum (FWHM) of the ($\bar{2}$ 01) substrate is 43 arcsec, indicating excellent bulk crystal quality. Figure 2(e) shows the cross-sectional image of the heterojunction between β-Ga_2O_3 and p-GaN. The high-resolution transmission electron microscopy (TEM) image shows the excellent quality of the exfoliated β-Ga_2O_3 flake after fabrication with p-GaN. Figure 2(g) shows a selected area electron diffraction (SAED) pattern of the exfoliated flake. The distance between (200) and (002) planes was found to be 0.56 nm and 0.275 nm, respectively. These

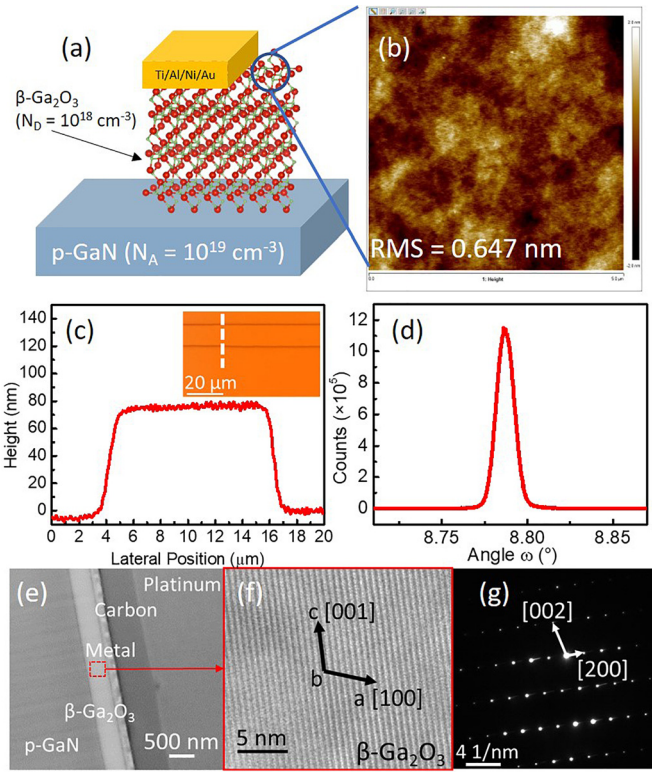

FIG. 2. Characterization of an exfoliated β-Ga_2O_3 flake. (a) Schematic of the exfoliated β-Ga_2O_3 sample. (b) AFM image of the exfoliated β-Ga_2O_3 flake (without metal). (c) Height profile of a mechanically exfoliated flake. No metal is present on this flake. (d) XRD Rocking curve for the $(\bar{2}01)$ bulk substrate. (e) Cross-sectional image of the heterojunction. (f) High-resolution TEM image of the mechanically exfoliated β-Ga_2O_3 flake. (g) SAED pattern of the mechanically exfoliated β-Ga_2O_3 flake.

values are highly consistent with previous works.[1,28,36,37] These results confirm that the flake was exfoliated along the (100) plane.

A typical I-V characteristic of the heterojunction is shown in Fig. 3(a) measured using a Keithley 2410 source meter for a 100 nm exfoliated β-Ga_2O_3 flake. When a forward bias was applied to the heterojunction, the device showed rectifying behaviors and the current began to increase after the turn-on voltage. The turn-on voltage is defined as the voltage value at which significant current (1×10^{-5} A) starts to flow. The device showed a decent rectification property with a rectification ratio of $\sim 10^5$, as shown in the inset of Fig. 3(a). During the transfer process, it is possible that the electrode metal on the β-Ga_2O_3 flake may accidently contact with p-GaN to form a Schottky diode. To rule out this possibility, the I-V characteristic of the p-GaN Schottky diode on the same wafer was tested. The comparison curve in Fig. 3(b) and its inset shows a drastic difference between the heterojunction and the Schottky barrier, with large disparity in turn-on voltage and reverse leakage. The p-GaN Schottky diode has a turn-on voltage of 1.3 V and three orders of magnitude larger leakage current. This indicates that the p-n heterojunction between β-Ga_2O_3 and p-GaN was indeed formed. Furthermore, a commercial software package, Silvaco, was used to simulate the energy band diagram for the p-n heterojunction. See Fig. 3(c). To extract the band structure,

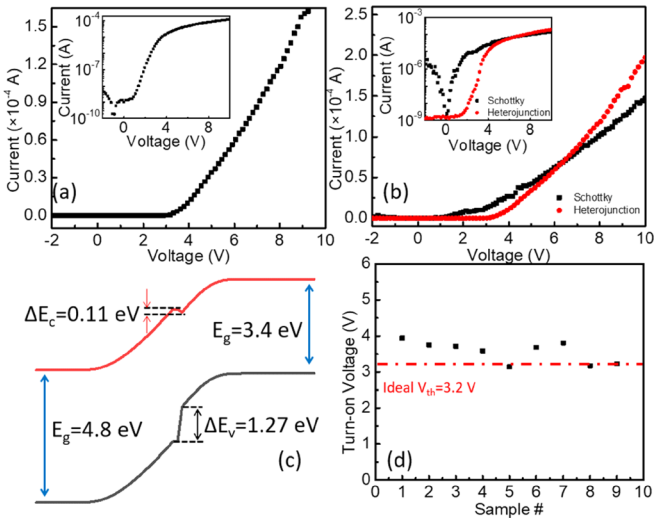

FIG. 3. (a) I-V characteristic of the 100 nm-thick exfoliated β-Ga_2O_3/p-GaN heterojunction (inset: logarithmic scale). (b) I-V comparison of the PN junction with a Schottky barrier diode (inset: logarithmic scale). (c) Band diagram simulated by Silvaco. (d) Turn-on voltage in a series of samples.

we defined the β-Ga_2O_3 and p-GaN materials using their respective bandgaps of 4.85 and 3.4 eV and respective doping concentrations as $N_D = 5 \times 10^{18}\ cm^{-3}$ and $N_A = 10^{19}\ cm^{-3}$. The electron affinity of β-Ga_2O_3 was set at 4.0 eV.[38] The local conduction band density of states was estimated to be $3.72 \times 10^{18}\ cm^{-3}$ based on an electron effective mass of $0.28m_0$.[39] Using these parameters along with Silvaco's own built-in material properties for p-GaN, we were able to extract the bandgap structure for the β-Ga_2O_3/p-GaN heterojunction. The band structure showed valence and conduction band offsets of 1.27 and 0.11 eV, respectively, which is consistent with the experiment results by X-ray photoelectron spectroscopy.[40] The simulated ideal turn-on voltage was 3.2 V. Figure 3(d) shows a comparison between the several measured and simulated turn-on voltages. The two values are comparable, confirming that the exfoliated β-Ga_2O_3 formed a heterojunction diode with p-GaN. The slightly larger measured turn-on voltages may be due to the existence of series resistance and defects, which are not taken into consideration in the simulation.

Owing to the heavily doped materials used in this diode ($n = 5 \times 10^{18}\ cm^{-3}$ and $p = 10^{19}\ cm^{-3}$), there is a possibility to form a tunneling diode. Tunneling diodes typically exhibit a very narrow depletion region and exceedingly low turn-on voltages.[41] Furthermore, the forward I-V characteristic in a tunneling diode exhibits a large initial tunneling current at low biases followed by a region of negative resistance. The width of the depletion region for the diode in this study was calculated to be 37.1 nm, which is extremely wide for tunneling. Examining the diode turn-on voltages in Fig. 3(d), we can see that tunneling is not a possibility, since the turn-on voltages in tunneling diodes are very low, usually lower than 1 V. In short, the tunneling mechanism was not observed in our devices. Figure 4(a) presents the temperature-dependent I-V characteristics of the β-Ga_2O_3/p-GaN heterojunction from 25 °C to 200 °C. The heterojunction showed good rectifying behaviors and thermal stability even at 200 °C. The general diode equations for current transport in a p-n junction can be expressed as[41]

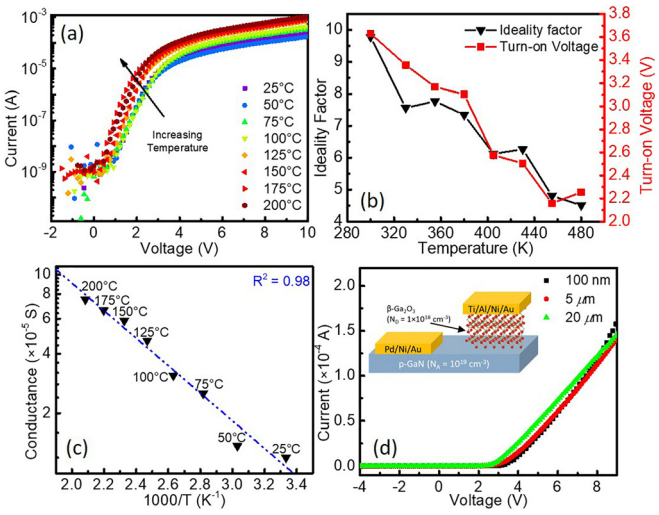

FIG. 4. Performance of the p-GaN/β-Ga_2O_3 diode with respect to temperature. (a) High temperature I-V characteristic of the 100 nm β-Ga_2O_3 p-n junction. (b) Turn-on voltage and ideality factors. (c) Electrical conductance at 3.5 V from 25 °C to 200 °C. (d) I-V characteristics of diodes as a function of different thicknesses.

$$I = I_s exp\left(\frac{qV}{nkT} - 1\right), \tag{1}$$

$$I_S = Aqn_i^2\left(\frac{D_p}{L_p N_D} + \frac{D_n}{L_n N_A}\right), \tag{2}$$

where I_s is the reverse saturation current, q is the electronic charge, V is the applied voltage, n is the ideality factor, k is the Boltzmann constant, T is the temperature, A is the diode area, D_p and D_n are the hole and electron diffusion coefficients (respectively), L_p and L_n are the hole and electron diffusion lengths (respectively), and N_D and N_A are the doping concentrations of the n and p layers (respectively). From (1), we can determine the saturation current as well as the ideality factor. As shown in Fig. 4(b), with increasing temperature, the ideality factor decreased from 9.8 to 4.5 and turn-on voltage decreased from 3.6 to 2.3 V. The decrease in turn-on voltages is due to the enhanced diffusion current across the p-n heterojunction with increasing temperatures. Figure 4(c) presents an Arrhenius plot of the conductance as a function of temperature at a forward bias of 3.5 V, where an improvement in conductivity is seen with increasing temperature. The activation energy estimated from Fig. 4(c) is 135 meV over the temperature range considered. In β-Ga_2O_3 as well as most oxides, the n-type conductivity arises due to the deep-donor oxygen vacancies, which activate at elevated temperatures.[42–44] However, the doping concentrations used in this study are $N_D = 5 \times 10^{18}$ cm^{-3} and $N_A = 10^9$ cm^{-3}; thus, the contribution of oxygen vacancies to conduction is likely minimal. In semiconductors, the intrinsic carrier concentration, n_i, increases with temperature. This in turn leads to an increase in the saturation current which increases the total current. This explains the increase in conductivity with temperature in Fig. 4(c). In addition, more β-Ga_2O_3/p-GaN diodes were formed with varying β-Ga_2O_3 thicknesses. Figure 4(d) presents the I-V characteristics of the p-n junction with β-Ga_2O_3 thicknesses of 100 nm, 5 μm, and 20 μm. Similar electrical characteristics are obtained across the various thicknesses.

We demonstrated a p-n heterojunction constructed between mechanically exfoliated β-Ga_2O_3 and p-GaN. The mechanical exfoliation process was described in detail and can be used for developing more advanced device structures. The electrical characteristics of the heterojunction were tested with I-V and temperature measurements. The formation of the p-n heterojunction between β-Ga_2O_3 and p-GaN was confirmed by both experiments and simulations. With increasing temperature, a decrease in both the ideality factor and turn-on voltage was observed. The heterojunction showed good thermal stability up to 200 °C. In addition, as the thicknesses of the β-Ga_2O_3 flakes increased, the device's electrical performance remained consistent. This work can serve as an important reference for future devices based on the heterojunction of exfoliated β-Ga_2O_3 and GaN for DUV, high-power, and high temperature applications.

This work was supported by the ARPA-E PNDIODES Program monitored by Dr. Isik Kizilyalli and partially supported by the NASA HOTTech Program Grant No. 80NSSC17K0768. We acknowledge the use of facilities within the Eyring Materials Center at Arizona State University. The device fabrication was performed at the Center for Solid State Electronics Research at Arizona State University. Access to the NanoFab was supported, in part, by NSF Contract No. ECCS-1542160.

REFERENCES

[1]G. Shin, H. Y. Kim, and J. Kim, Korean J. Chem. Eng. **35**, 574 (2018).
[2]M. Orita, H. Ohta, M. Hirano, and H. Hosono, Appl. Phys. Lett. **77**, 4166 (2000).
[3]M. Higashiwaki, K. Sasaki, H. Murakami, Y. Kumagai, A. Koukitu, A. Kuramata, T. Masui, and S. Yamakoshi, Semicond. Sci. Technol. **31**, 034001 (2016).
[4]H. He, R. Orlando, M. A. Blanco, R. Pandey, E. Amzallag, I. Baraille, and M. Rerat, Phys. Rev. B **74**, 195123 (2006).
[5]M. A. Mastro, A. Kuramata, J. Calkins, J. Kim, F. Ren, and S. Pearton, ECS J. Solid State Sci. Technol. **6**, P356 (2017).
[6]S. J. Pearton, J. Yang, P. H. Cary, IV, F. Ren, J. Kim, M. J. Tadjer, and M. A. Mastro, Appl. Phys. Rev. **5**, 011301 (2018).
[7]H. Chen, H. Fu, X. Huang, J. Montes, T. Yang, I. Baranowski, and Y. Zhao, Opt. Express **26**, 3938 (2018).
[8]H. Fu, H. Chen, X. Huang, I. Baranowski, J. Montes, T. Yang, and Y. Zhao, IEEE Trans. Electron Devices **65**(8), 3507 (2018).
[9]H. Chen, H. Fu, X. Huang, J. Montes, T. Yang, I. Baranowski, and Y. Zhao, eprint arXiv:1712.01390 (2017).
[10]J. Y. Tsao, S. Chowdhury, M. A. Hollis, D. Jena, N. M. Johnson, K. A. Jones, R. J. Kaplar, S. Rajan, C. G. Van De Walle, E. Bellotti, C. L. Chua, R. Collazo, M. E. Coltrin, J. A. Cooper, K. R. Evans, S. Graham, T. A. Grotjohn, E. R. Heller, M. Higashiwaki, M. S. Islam, P. W. Juodawlkis, M. A. Khan, A. D. Koehler, J. H. Leach, U. K. Mishra, R. J. Nemanich, R. C. N. Pilawa-Podgurski, J. B. Shealy, Z. Sitar, M. J. Tadjer, A. F. Witulski, M. Wraback, and J. A. Simmons, Adv. Electron. Mater. **4**, 1600501 (2018).
[11]G. Yang, S. Jang, F. Ren, S. J. Pearton, and J. Kim, ACS Appl. Mater. Interfaces **9**, 40471 (2017).
[12]J. Åhman, G. Svensson, and J. Albertsson, Acta Crystallogr., Sect. C **52**, 1336 (1996).
[13]K. Bourzac, technologyreview.com/s/421072/graphene-wins-nobel-prize/ for "2010 Nobel Prize awarded to Andre Geim and Konstantin Novoselov for graphene research" (last accessed November 28, 2018).
[14]P. Goli, J. Khan, D. Wickramaratne, R. K. Lake, and A. A. Balandin, Nano Lett. **12**, 5941 (2012).
[15]J. Khan, C. M. Nolen, D. Teweldebrhan, D. Wickramaratne, R. K. Lake, and A. A. Balandin, Appl. Phys. Lett. **100**, 043109 (2012).
[16]Y. Kwon, G. Lee, S. Oh, J. Kim, S. J. Pearton, and F. Ren, Appl. Phys. Lett. **110**, 131901 (2017).

[17]R. Mitdank, S. Dusari, C. Bülow, M. Albrecht, Z. Galazka, and S. F. Fischer, Phys. Status Solidi A **211**, 543 (2014).
[18]W. Mu, Z. Jia, Y. Yin, Q. Hu, J. Zhang, Q. Feng, Y. Hao, and X. Tao, CrystEngComm **19**, 5122 (2017).
[19]A. Li, Q. Feng, J. Zhang, Z. Hu, Z. Feng, K. Zhang, C. Zhang, and H. Zhou, Superlattices Microstruct. **119**, 212 (2018).
[20]M. J. Tadjer, N. Mahadik, V. Wheeler, E. Glaser, L. Ruppalt, A. Koehler, K. Hobart, C. Eddy, and F. Kub, ECS J. Solid State Sci. Technol. **5**(9), P468 (2016).
[21]W. Hwang, A. Verma, H. Peelaers, V. Protasenko, S. Rouvimov, H. Xing, A. Seabaugh, A. Haensch, C. V. Walle, Z. Galazka, M. Albrecht, R. Fornari, and D. Jena, Appl. Phys. Lett. **104**, 203111 (2014).
[22]H. Zhou, M. Si, S. Alghamdi, G. Qiu, L. Yang, and P. Ye, IEEE Electron Device Lett. **38**, 103 (2017).
[23]H. Zhou, K. Maize, G. Qiu, A. Shakouri, and P. Ye, Appl. Phys. Lett. **111**, 092102 (2017).
[24]J. Bae, H. Kim, I. H. Kang, G. Yang, and J. Kim, Appl. Phys. Lett. **112**, 122102 (2018).
[25]J. Son, Y. Kwon, J. Kim, and J. Kim, ECS J. Solid State Sci. Technol. **7**, Q148 (2018).
[26]Z. Li, Y. Liu, A. Zhang, Q. Liu, C. Shen, F. Wu, C. Xu, M. Chen, H. Fu, and C. Zhou, Nano Res. **12**, 143 (2019).
[27]S. Oh, J. Kim, F. Ren, S. J. Pearton, and J. Kim, J. Mater. Chem. C **4**, 9245 (2016).
[28]S. Oh, M. Mastro, M. Tadjer, and J. Kim, ECS J. Solid State Sci. Technol. **6**, Q79 (2017).
[29]A. Kyrtsos, M. Matsubara, and E. Bellotti, Appl. Phys. Lett. **112**, 032108 (2018).
[30]J. Robertson and S. Clark, Phys. Rev. B **83**, 075205 (2011).
[31]J. Varley, J. Weber, A. Janotti, and C. G. Van de Walle, Appl. Phys. Lett. **97**, 142106 (2010).
[32]S. Lany and A. Zunger, Phys. Rev. B **80**, 085202 (2009).
[33]A. Stoneham, J. Gavartin, A. Shluger, A. Kimmel, D. Ramo, H. Rønnow, G. Aeppli, and C. Renner, J. Phys. Condens. Matter **19**, 255208 (2007).
[34]J. Varley, A. Janotti, C. Franchini, and C. G. Van de Walle, Phys. Rev. B **85**, 081109 (2012).
[35]K. Iizuka, Y. Morishima, A. Kuramata, Y. Shen, C. Tsai, Y. Su, G. Liu, T. Hsu, and J. H. Yeh, Proc. SPIE **9363**, 93631Z (2015).
[36]J. Kim, S. Oh, M. A. Mastro, and J. Kim, Phys. Chem. Chem. Phys. **18**, 15760 (2016).
[37]J. Kim, M. Mastro, M. Tadjer, and J. Kim, ACS Appl. Mater. Interfaces **9**, 21322 (2017).
[38]M. Mohamed, K. Irmscher, C. Janowitz, Z. Galazka, R. Manzke, and R. Fornari, Appl. Phys. Lett. **101**, 132106 (2012).
[39]K. Irmscher, Z. Galazka, M. Pietsch, R. Uecker, and R. Fornari, J. Appl. Phys. **110**, 063720 (2011).
[40]W. Wei, Z. Qin, S. Fan, Z. Li, K. Shi, Q. Zhu, and G. Zhang, Nanoscale Res. Lett. **7**, 562 (2012).
[41]S. M. Sze and K. K. Ng, *Physics of Semiconductor Devices*, 3rd ed. (Wiley, New York, 2006).
[42]A. Neal, S. Mou, R. Lopez, J. Li, D. Thomson, K. Chabak, and G. Jessen, Sci. Rep. **7**, 13218 (2017).
[43]Y. Tomm, J. Ko, A. Yoshikawa, and T. Fukuda, Sol. Energy Mater. Sol. Cells **66**, 369 (2001).
[44]Z. Hajnal, J. Miró, G. Kiss, F. Réti, P. Deák, R. Herndon, and J. Kuperberg, J. Appl. Phys. **86**, 3792 (1999).